 

PACS numbers: 42.55.Px; 78.67.De; 78.20.Ls
DOI: 10.1070/QE2013v043n02ABEH015077

# Broadening and splitting of emission spectra of a GaInAs/AlInAs quantum cascade laser in a quantising magnetic field

I.I. Zasavitskii, D.A. Pashkeev, E.V. Bushuev, G.T. Mikaelyan

*Abstract.* **We have studied the effect of a relatively weak quantising magnetic field on emission spectra of a GaInAs/AlInAs quantum cascade laser near 10 K. The results demonstrate that, as the magnetic field induction increases to 7 T, the spectra broaden (to 5 meV) and split into three emission bands. As a result, we observe simultaneously up to 80 longitudinal lasing modes in the three bands and the integrated laser output intensity increases 70 times. The presence of bands in the emission spectra can be accounted for in terms of the magnetic quantisation of the laser levels into spin-split Landau levels. The increase in emission intensity is attributable primarily to phonon resonance adjustment in a magnetic field.**

***Keywords:*** *quantum cascade laser, quantum well, barrier, quantising magnetic field, splitting of emission spectra, GaInAs/AlInAs system.*

The quantum cascade laser (QCL) is a unipolar semiconductor device based on intersubband transitions in a quantum-confined heterostructure. Such lasers operate in the near-IR (3–24 μm) and far-IR (70–250 μm) spectral regions and employ mainly the GaInAs/AlInAs and GaAs/AlGaAs systems, respectively. The effect of a strong magnetic field (up to 40 T) was studied primarily for terahertz GaAs/AlGaAs QCLs (see Wade et al. [1] and references therein) and, to a lesser extent, for GaInAs/AlInAs QCLs [2–4] emitting in the 10-μm range. In the latter material system, the electrons in the GaInAs quantum well have a relatively small effective mass and considerable $g$-factor, which reduces the magnetic quantisation threshold.

This paper addresses the effect of a quantising magnetic field on emission spectra ($\lambda \approx 9$ μm) of a GaInAs/AlInAs QCL near 10 K.

The influence of an external quantising magnetic field on the output of a QCL provides an effective tool for controlling the energy spectrum and lifetime of nonequilibrium charge carriers in both radiative recombination and various nonradiative recombination channels. Indeed, a strong magnetic field applied to a quantum-confined heterostructure across its plane, i.e. along its growth direction, leads to additional magnetic quantisation. If the dispersion law $E(k)$ of a deep quantum well in zero magnetic field in the parabolic approximation has the form

$$E(k) = E_n + \frac{\hbar^2 k_\perp^2}{2m^*} = \frac{\pi\hbar^2 n^2}{2m^* L_z^2} + \frac{\hbar^2 k_\perp^2}{2m^*} \quad (1)$$

(where $m^*$ is the electron effective mass; $L_z$ is the quantum well width; and $n$ is the size quantum number) and electron motion with a wave vector $k_\perp$ is free in the plane of the structure, then a quantising magnetic field $B$ splits each two-dimensional (2D) subband into a series of equally spaced discrete Landau levels,

$$E_{n,l} = E_n + \hbar\omega_c\left(l + \frac{1}{2}\right) \quad (2)$$

(where $l = 0, 1, 2, 3\ldots$ is the Landau level number), separated by the cyclotron energy, $\hbar\omega_c = eB/(m^*c)$. When the charge carriers have a large effective $g$-factor, also important is the spin splitting of the Landau levels by $g\beta B$, where $\beta$ is the Bohr magneton. Thus, in the limit of sufficiently large magnetic fields, the 2D density of states takes the form of a delta function, corresponding to a quantum dot, because of the magnetic confinement.

Such radical changes in the energy spectrum of the quantum well lead to significant changes in its properties, in particular to a shift of the quantum well levels in the QCL, which disturbs their fine-tuned spectrum and, hence, laser operation. Also possible is the opposite situation: the levels can be tuned by a magnetic field for successful QCL operation. There is also a change in matrix element, which eventually influences laser operation. Consequently, scanning a strong magnetic field, one can obtain various states corresponding to QCL output intensity oscillations. The magnetic field effect on the QCL output was studied previously in very strong static (up to 30 T) and pulsed (up to 40 T) magnetic fields, i.e. at cyclotron energies comparable to (at $B \approx 15$ T) or higher than the longitudinal optical (LO) phonon energy [1–4]. Clearly, the oscillation pattern depends on the particular design scheme and materials parameters of the QCL.

In this study, the active region of a laser heterostructure consisted of four quantum wells, which ensured two-phonon depopulation of the lower laser level [5]. Figure 1 shows the calculated energy band diagram of the active region in a QCL. The calculation was made in the envelope function and effective mass approximations using a single-band model. The arrow represents the laser transition between the levels with energies $E_5$ and $E_3$. Levels $E_1$ and $E_2$ are separated from the lower laser level $E_3$ by two LO phonon energies and one LO phonon energy (35 meV in $Ga_{0.47}In_{0.53}As$), respectively. Level $E_4$ corresponds to the ground state of the injector. Level $E_6$ is the nearest to the upper laser level $E_5$ and is separated from it

**I.I. Zasavitskii, D.A. Pashkeev, E.V. Bushuev** P.N. Lebedev Physics Institute, Russian Academy of Sciences, Leninsky prosp. 53, 119991 Moscow, Russia; e-mail: zasavit@sci.lebedev.ru;
**G.T. Mikaelyan** OJSC Research and Manufacturing Enterprise 'Inject', prosp. 50-letiya Oktyabrya 101, 410052 Saratov, Russia

Received 10 December 2012
*Kvantovaya Elektronika* **43** (2) 144–146 (2013)
Translated by O.M. Tsarev

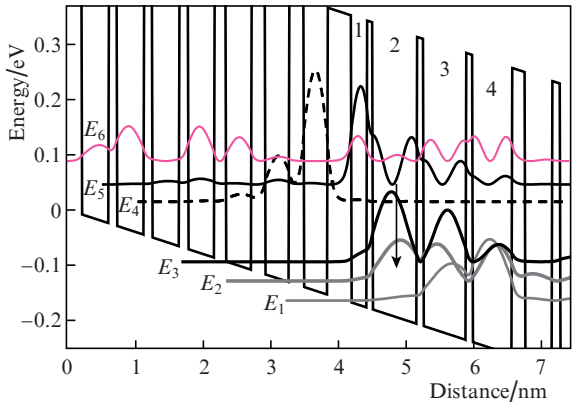


**Figure 1.** Calculated energy band diagram of a four-well (1–4) active region in a QCL at an electric field strength of 40 kV cm$^{-1}$.

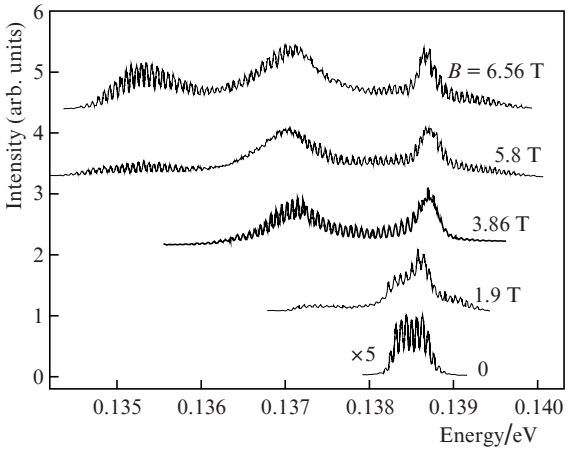


**Figure 2.** Magnetic field effect on the 10-K emission spectrum of the QCL at a 8-A current through the sample.

by 43 eV. It can, in principle, reduce the population of level $E_5$, but its role at low temperatures ($k_0T \approx 0.86$ meV at 10 K) is insignificant.

The $Ga_{0.47}In_{0.53}As/Al_{0.48}In_{0.52}As/InP$ laser heterostructure was grown at the University of Sheffield (United Kingdom) by metalorganic vapour phase epitaxy on an n-InP(100) substrate with an electron concentration above $2 \times 10^{18}$ cm$^{-3}$ [6, 7]. The thicknesses (in angstroms) of the quantum wells and barriers (bold), starting from the injection barrier, were **35**/23/**8**/66/**9**/64/**9**/58/**20**/40/**12**/40/**12**/40/**13**/39/**17**/38/**21**/35/**22**/35. The thicknesses of the injector layers doped with silicon to $\sim 1 \times 10^{17}$ cm$^{-3}$ are underlined. The structure contained 35 stages, sandwiched between n-InP cladding layers about 3 μm thick, with a doping level of $1 \times 10^{17}$ cm$^{-3}$. The upper InP contact layer had a stepwise doping profile with the highest concentration of $1 \times 10^{19}$ cm$^{-3}$. Using photolithography, 50-μm-wide longitudinal mesa stripes were produced by etching, resulting in the formation of a ridge (stripe) waveguide with a resonator length of 3 mm. After standard contacts were made, the laser chips were indium-soldered epi-down to alloy MD-50, which was in turn soldered to a copper holder [8]. This allowed high currents to be passed through the sample and alleviated the problem of stress at liquid helium temperatures due to the thermal expansion mismatch.

The lasers were mounted in the Voigt configuration ($\boldsymbol{k} \perp \boldsymbol{B}$) in a superconducting solenoid placed in an optical cryostat with KCl windows [9]. The sample temperature was within 10 K, and the highest magnetic field was 7 T. The lasers were operated with 0.5-μs current pulses at a 170-Hz repetition rate. We used a grating monochromator (75 lines mm$^{-1}$) and a Ge:Cu detector with a red limit at 28 μm. The energy resolution was 0.02 meV at a wavelength of 9 μm.

Figure 2 shows high-resolution emission spectra of the QCL in different magnetic fields. It is worth noting that, with increasing magnetic field, the integrated emission intensity increases. Special measurements showed that the integrated emission intensity at $B = 7$ T was 70 times that in zero magnetic field. This was caused to a significant degree by the broadening of the emission spectrum, primarily towards lower energies. A second emission band emerges at $B$ as low as 2 T, and a third band emerges at $B = 5$ T. The total lasing range reaches 5 meV (40 cm$^{-1}$). The three emission bands have a well-defined mode structure with equally spaced peaks corresponding to a separation between longitudinal modes $\Delta k = (2NL)^{-1} \approx 0.5$ cm$^{-1}$, where $L = 3$ mm is the resonator length and $N \approx 3.3$ is the effective refractive index of the active medium.

Figure 3 illustrates the magnetic field effect on the energy position of the emission bands. As seen, the data for the $T_1$ and $T_2$ bands are well represented by straight lines with a negative slope ($-4.5 \times 10^{-4}$ and $-1.8 \times 10^{-4}$ eV T$^{-1}$, respectively). The magnetic field dependence for the $T_3$ band has a positive slope ($1.9 \times 10^{-4}$ eV T$^{-1}$) in low fields and becomes relatively weak for $B \geqslant 5$ T. The inset in Fig. 3 shows a tentative diagram of optical transitions: the $T_1$ and $T_3$ bands correspond to spin flip transitions and the $T_2$ band is due to quasi-degenerate spin-conserved transitions.

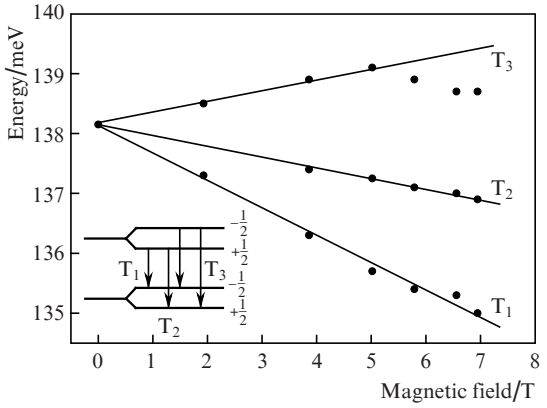


**Figure 3.** Magnetic field effect on the energy position of the emission bands $T_1$–$T_3$. Inset: diagram of possible transitions between spin-split zero-energy Landau levels.

We calculated the slope for the $T_1$–$T_3$ bands with allowance for effective-mass and $g$-factor nonparabolicity. The effective-mass nonparabolicity was represented in the form $m^* = m_0(1 + E/E_g)$, where $m_0$ is the mass at the conduction band bottom and $E_g$ is the band gap. Even though $Ga_{0.47}In_{0.53}As$ has a small $g$-factor ($g = -4.2$), the spin splitting in it amounts to about 10% of the cyclotron energy. In our calculations, we took into account this and its variation with magnetic field: $g = g_0 - C(1 + 1/2)B$, where $C = 0.069$ T$^{-1}$

[10]. As a result, we obtained slopes of (–4.2, –1.9 and 0.3) × $10^{-4}$ eV $T^{-1}$ for the $T_1$, $T_2$ and $T_3$ transitions, respectively. Thus, there is good agreement between the calculated and measured slopes only for the spin flip transitions ($T_1$) and quasi-degenerate spin-conserved transitions ($T_2$). As to the other line ($T_3$) corresponding to spin flip transitions, it follows from theory that it should be a weak function (of the same order as the nonparabolicity) of magnetic field, whereas according to our experimental data its energy position is an intricate function of magnetic field.

The strong magnetic field dependence of the integrated laser output intensity can be accounted for by several factors. In addition to the above-mentioned broadening of the emission spectrum (basically the formation of extra lasing channels from spin-split Landau levels), it is worth mentioning the slight increase, proportional to $\sqrt{B}$, in the density of states in a magnetic field and the magnetic tuning of resonances. In the latter case, we mean the slight decrease in the energy separation between the injector ground level $E_4$ and the upper laser level $E_5$ (Fig. 1). The most important factor, however, is the magnetic tuning of resonance transitions between the $E_1$, $E_2$ and $E_3$ levels. According to calculations for the laser heterostructure under consideration, these energy separations at $B = 0$ ($E_3 - E_2 = 36.2$ meV and $E_2 - E_1 = 35.5$ meV) differ very little from the LO phonon energy (35 meV in GaInAs). QCL-type devices are more reliable when these energy separations slightly exceed the LO phonon energy. Further work is needed to fully understand the origin of the magnetic-field-induced sharp increase in emission intensity. In addition, it is necessary to study the electroluminescence of the device and measure the polarisation of the observed emission bands in a magnetic field, because the observed polarisation of the emission spectra of the QCL is strongly suppressed by the preset laser output polarisation (parallel to the growth plane).

Thus, in a relatively weak quantising magnetic field, the emission spectrum of a GaInAs/AlInAs QCL broadens (to 5 meV) and splits into three emission bands. As a result, we observe simultaneously up to 80 longitudinal lasing modes in the three bands and the integrated laser output intensity increases 70 times. The presence of bands in the emission spectrum can be accounted for in terms of the magnetic quantisation of the laser levels into spin-split Landau levels, and the increase in intensity is attributable to phonon resonance adjustment in a magnetic field. The broadening of lasing spectra in a quantising magnetic field can be used for wavelength tuning in external cavity lasers [11].

***Acknowledgements.*** We are grateful to A.B. Krysa for growing the laser heterostructure.

This work was supported by the Russian Foundation for Basic Research (Grant No. 11-02-00980-a).

## References

1. Wade A., Fedorov G., Smirnov D., Kumar S., Williams B.S., Hu Q., Reno J.L. *Nat. Photonics*, **3**, 41 (2009).
2. Blaser S., Diehl L., Beck M., Faist J. *Phys. E*, **7**, 33 (2000).
3. Vasanelli A., Leuliet A., Sirtori C., Wade A., Fedorov G., Smirnov D., Bastard G., Vinter B., Giovannini M., Faist J. *Appl. Phys. Lett*., **89**, 172120 (2006).
4. Semtsiv M. P., Dressler S., Masselink W. T., Fedorov G., Smirnov D. *Appl. Phys. Lett*., **89**, 171105 (2006).
5. Faist J., Hofstetter D., Beck M., Aellen T., Rochat M., Blaser S. *IEEE J. Quantum Electron*., **38**, 533 (2002).
6. Krysa A.B., Roberts J.S., Green R.P., Wilson L.R., Page H., Garsia M., Cockburn J.W. *J. Cryst. Growth*, **272**, 682 (2004).
7. Green R.P., Krysa A., Roberts J.S., Revin D.G., Wilson L.R., Zibik E.A., Ng W.H., Cockburn J.W. *Appl. Phys. Lett*., **83**, 1921 (2003).
8. Zasavitskii I.I., Pashkeev D.A., Marmalyuk A.A., Ryaboshtan Yu.L., Mikaelyan G.T. *Kvantovaya Elektron*., **40**, 95 (2010) [*Quantum Electron*., **40**, 95 (2010)].
9. Gureev D.M., Zasavitskii I.I., Matsonashvili B.N. *Prib. Tekh. Eksp*., **3**, 242 (1978).
10. Dobers M., Vieren J.P., Guldner Y., Bove P., Omnes F., Razeghi M. *Phys. Rev. B*, **40**, 8075 (1989).
11. Hugi A., Maulini R., Faist J. *Semicond. Sci. Technol*., **25**, 083001 (2010).